The EMBO Journal Vol. 22 No. 9 pp. 1959–1968, 2003

NEW EMBO MEMBER'S REVIEW

Ferritins, iron uptake and storage from the bacterioferritin viewpoint

Maria Arménia Carrondo[1]

Instituto de Tecnologia Química e Biológica, Universidade Nova de Lisboa, Av. República, 2784-505 Oeiras, Portugal

[1]Corresponding author
e-mail: carrondo@itqb.unl.pt

Ferritins constitute a broad superfamily of iron storage proteins, widespread in all domains of life, in aerobic or anaerobic organisms. Ferritins isolated from bacteria may be haem-free or contain a haem. In the latter case they are called bacterioferritins. The primary function of ferritins inside cells is to store iron in the ferric form. A secondary function may be detoxification of iron or protection against O_2 and its radical products. Indeed, for bacterioferritins this is likely to be their primary function. Ferritins and bacteroferritins have essentially the same architecture, assembling in a 24mer cluster to form a hollow, roughly spherical construction. In this review, special emphasis is given to the structure of the ferroxidase centres with native iron-containing sites, since oxidation of ferrous iron by molecular oxygen takes place in these sites. Although present in other ferritins, a specific entry route for iron, coupled with the ferroxidase reaction, has been proposed and described in some structural studies. Electrostatic calculations on a few selected proteins indicate further ion channels assumed to be an entry route in the later mineralization processes of core formation.

Keywords: bacterioferritins/ferroxidase activity/iron storage/native di-iron centres/specific iron channel

Introduction

Iron is essential for the growth and development of most organisms. It is one of the most abundant metals in the Earth's crust. It possesses two stable oxidation states (II) and (III) that are readily interchangeable, thus allowing iron to participate in redox reactions covering a wide range of potentials (Andrews, 1998). This flexibility makes it an extremely useful redox mediator in biology. Furthermore, the several spin states available for iron ions allow it to act as a catalyst in reactions involving molecular oxygen. As a result, it is involved in a variety of critical processes on which life depends, such as respiration, DNA synthesis, nitrogen fixation and photosynthesis. However, with the advent of an oxygen-rich atmosphere, oxidation of the initial ferrous ion pool to the ferric form created two problems. Fe(II) activates dioxygen, with the general production of intermediate reactive species causing serious hazards through oxidative damage processes, thus preventing its use as an available iron source. On the other hand, Fe(III) has a low solubility under physiological conditions (~10^{-18} M), requiring living organisms to adapt more efficient iron storage/transport/usage mechanisms.

A means of iron storage is thus required, and ferritins fulfil this role in organisms as diverse as bacteria, fungi, plants and vertebrates. Their wide distribution among living species implies a fundamental and ancient role in iron metabolism. Iron is present within the cells of living organisms either complexed in iron-containing proteins and enzymes or in iron-storage proteins. It can be incorporated in protein molecules in the form of a haem, bound to sulfur in various types of iron–sulfur clusters, in mixed-metal centres (e.g. containing nickel), as di-iron or as mononuclear iron centres (Crichton, 2001).

Basic roles of ferritins

Ferritins constitute a broad superfamily of iron-storage proteins, widespread in the three kingdoms of life, in aerobic or anaerobic organisms. Ferritins isolated from bacteria may also contain a haem b, and are then called bacterioferritins (Bfr). The basic role performed by ferritins is to supply cells with the necessary iron, leading to effective concentrations in living cells in the range of 10^{-3}–10^{-5} M. However, they can be also involved in cell redox-stress resistance.

Thus, ferritins have the unique feature of controlling the reversible phase transition between hydrated Fe(II) in solution and the solid mineral core inside its cavity (Theil, 2001). When iron concentrations are very high, ferritin also has a protective 'anti-oxidating' function by sequestering the iron inside the cavity, away from dioxygen, hydrogen peroxide and superoxide. Then ferritin assumes an iron detoxification function.

In anaerobic organisms or at anaerobic reaction centres in cells, ferritins and bacterioferritins can also assume a dioxygen detoxification role by consuming dioxygen through the ferroxidase reaction. The recent discovery of a new ferritin specific for the mitochondria suggests that this protein plays a role in the protection against oxidative damage, since almost all of the iron must pass through the mitochondria to become functionally active (Levi *et al*., 2001; Arosio and Levi, 2002).

Storage of iron is, therefore, the main function of ferritins. Detoxification of iron and dioxygen are secondary protective functions utilized under extreme conditions (Theil, 2001). However, it still remains to be proven whether these roles constitute the primary function of bacterioferritins.

X-ray structures of ferritins

Although there are a large number of ferritins with known amino acid sequence, X-ray structures of a relatively small number have been determined, namely: native horse

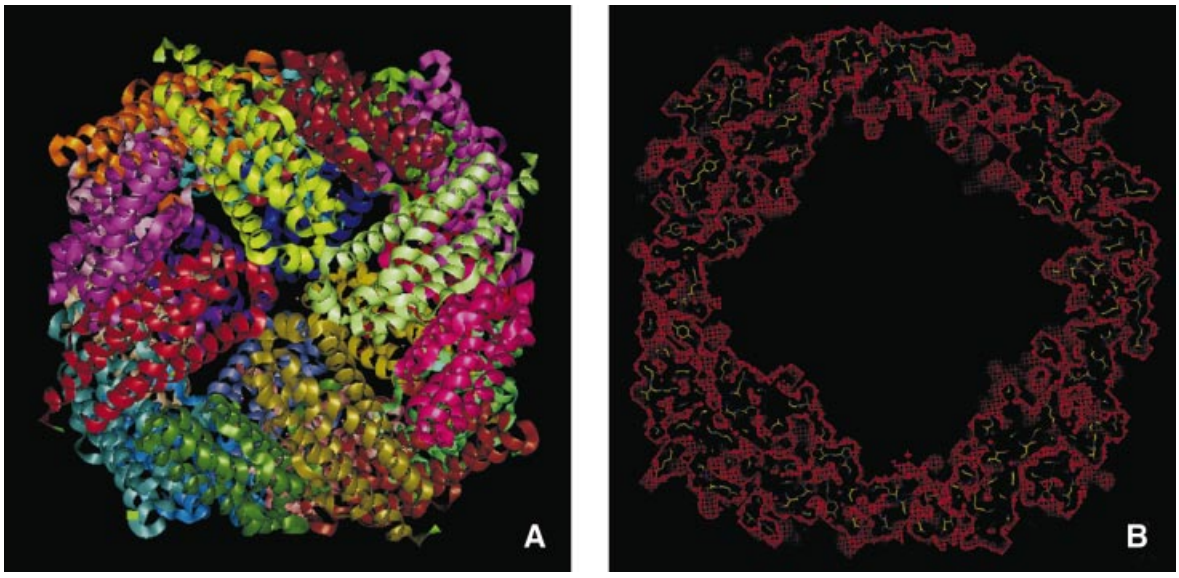

Fig. 1. (**A**) Overall view of the *Dd* Bfr [Protein Data Bank (PDB) access code 1nfv]. Different colours represent the 12 dimers. In (**B**), the mask (in red), highlighting the inner core, was calculated with the program MAMA (Kleywegt and Jones, 1999) with a 3 Å radius around all atoms.

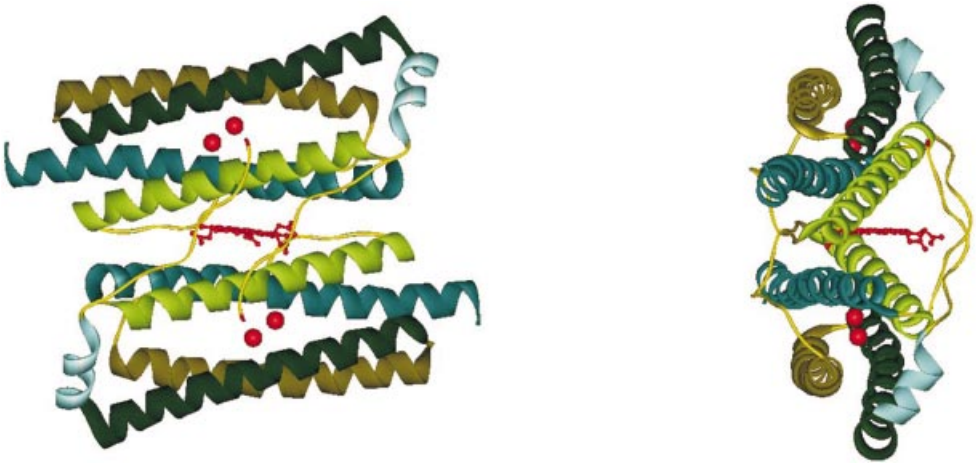

Fig. 2. Two subunits from the *Dd* Bfr forming one homodimer. The location of the Fe-coproporphyrin III haem in the 2-fold interface is shown. The red spheres represent the di-iron ferroxidase centres in each of the monomers.

spleen (Banyard *et al*., 1978; Rice *et al*., 1983), native rat liver (Lawson, 1990), recombinant rat L chain (Lawson, 1990), recombinant (Lawson *et al*., 1991) and variant (Hempstead *et al*., 1997) human H chain, recombinant bullfrog M (a second type of H chain) (Ha *et al*., 1999), L chain (Trikha *et al*., 1994) and variant H chain (Takagi *et al*., 1998), recombinant horse L chain (Gallois *et al*., 1997) and recombinant mouse L chain (Granier *et al*., 2001, 2003).

For bacteria, three bacterioferritin structures are known to date, from *Escherichia coli* (*Ec*) (Frolow *et al*., 1994; Dautant *et al*., 1998; Frolow and Kalb, 2001), *Rhodobacter capsulatus* (*Rc*) (Cobessi *et al*., 2002) and *Desulfovibrio desulfuricans* ATCC 27774 (*Dd*) (Macedo *et al*., 2003), and two haem-free ferritins, from *Ec* (Hempstead *et al*., 1994; Stillman *et al*., 2001) and *Listeria innocua* (*Li*) (Ilari *et al*., 2000).

Ferritins and bacteroferritins have essentially the same architecture, assembling in a 24mer cluster to form a hollow, roughly spherical, construction with a diameter ~120 Å (Figure 1). In general, the iron storage cavity has a diameter of ~80 Å and can accommodate up to 4500 iron ions as an inorganic complex core. Each subunit (~20 kDa) folds as a four α-helix bundle capped by a shorter helix at the C-terminal end. The 24 subunits are related by 4-, 3- and 2-fold symmetry axes (432-point symmetry). At the 3-fold axis there are channels that traverse the cavity. The subunits associate as dimers, and in bacterioferritins, the haem is located between the two subunits (Figure 2).

Mammalian ferritins consist of two types of subunits, H and L chains (heavy and light), only 55% identical in sequence but mutually interchangeable in the fully assembled 24mer molecule (Harrison *et al*., 1987). H or L chain contents vary according to the organ and its iron

requirements, and it appears that while H chains confer ferroxidase activity to the heteropolymer, L chains confer nucleation sites for iron binding. In general, H-rich ferritins are characteristic of brain and heart tissues, and have low iron content when compared with that of L-rich ferritins found in typical iron-storage organs (such as liver and spleen). Amphibian red cells contain three types of chain, H, L and M (medium), which can form heteropolymers.

Recently, an exception to the highly conserved architecture of ferritins has been found with the determination of the structure of *Li* ferritin to 2.35 Å resolution, which revealed a 12mer cluster related by 23 symmetry (Ilari *et al*., 2000). Another example of this type of arrangement was found with the structure of the ferritin homologue Dps (DNA-binding proteins from starved cells) from *Ec* (Grant *et al*., 1998) solved to 1.6 Å resolution. *Bacillus anthracis*, the agent causing the various forms of anthrax, possesses two different genes encoding for proteins (Dlp-1 and Dlp-2) with amino acid sequences similar to those of proteins belonging to this new class of ferritin-like bacterial proteins (Dps family). In a similar way to the *Ec* Dps, Dlp-1 and Dlp-2 are dodecamers of 12 identical subunits, generating a nearly spherical shell of a diameter of ~45 Å (Papinutto *et al*., 2002). Both Dlp-1 and Dlp-2 may act as ferritins, since they are able to bind and sequester free iron, allowing bacterial growth under iron overload conditions.

Presence of iron and the ferroxidase site

It is now well established that the uptake of iron by (bacterio)ferritins involves an initial step of oxidation by molecular oxygen of ferrous iron, through a binuclear di-iron centre, the ferroxidase centre (Le Brun *et al*., 1993, 1995; Pereira *et al*., 1998). A possible mechanism for aerobic oxidative uptake was proposed, assuming that three kinetically different phases are involved: Fe(II) binding at the ferroxidase centre, fast catalytic Fe(II) oxidation at the ferroxidase centre and entry of iron (III) into the core.

Additionally, the detection of a peroxo-differic intermediate in the ferritin ferroxidase reactions (Treffry *et al*., 1995; Zhao *et al*., 1997; Moenne-Loccoz *et al*., 1999; Hwang *et al*., 2000) as proposed years ago (Crichton and Roman, 1978), further established the di-iron centre as the ferroxidase site.

Ferritins and bacterioferritins are normally obtained from samples where the iron has been removed and thus only in some cases has the presence of iron been detected in their structures. This is the case for dodecameric ferritin from *Li* (Ilari *et al*., 2000) and the *Ec* ferritin (Hempstead *et al*., 1994; Stillman *et al*., 2001). In the former, one single iron atom was located at the interface between monomers, while in the second, three iron atoms per monomer (two forming a di-iron site) were inserted in the protein by soaking the crystals in a ferrous salt solution. In the *Ec* Bfr (Frolow *et al*., 1994; Dautant *et al*., 1998; Frolow and Kalb, 2001), the di-metal site is filled with two Mn^{2+} ions arising from the crystallization mother liquor, whereas in *Rc* Bfr structure (Cobessi *et al*., 2002) it has an iron with low occupancy.

Dd Bfr was the first bacterioferritin to be isolated with a 'native' di-iron ferroxidase centre. The presence of this centre in the 'as isolated sample' obtained from an anaerobic purification was first demonstrated by EPR data (Romão *et al*., 2000b). The EPR studies were consistent with the iron centres being in the di-ferric state. Furthermore, in contrast to all other isolated Bfrs, *Dd* Bfr has the further unique feature of having Fe-coproporphyrin III as its haem cofactor, the first example of such a haem in a biological system (Romão *et al*., 2000a). These biochemical and spectroscopic results were confirmed by the X-ray structure determination of *Dd* Bfr in three different catalytic states: to 1.95 Å resolution from an 'as isolated' protein sample anaerobically purified but aerobically crystallized; to 2.05 Å resolution from a sample prepared and crystallized as in the first case, but followed by reduction of the crystal with sodium dithionite; and to 2.35 Å resolution, from a 'cycled' oxidized sample, i.e. a sample that was fully reduced and subsequently allowed to re-oxidize by exposure to oxygen and crystallized aerobically. Initially, the structure of the 'as isolated' form was solved using the multiple-wavelength anomalous dispersion technique and X-ray wavelengths around the iron Kα edge. The haem molecules were located between pairs of monomers and are coordinated axially via symmetry-related Met57 residues. Within their plane, the haem molecules are disordered in a similar manner to that found in *Rc* Bfr and they have been modelled in two overlapping conformations so that the four propionate groups form hydrogen bonds with polypeptide residues.

The ferroxidase centre

The residues forming the di-iron centre in *Dd* Bfr are glutamates and histidines: Glu23, Glu56, Glu99 and Glu132, and His59 and His135. All these residues are mainly conserved in the bacterioferritin family. However, there are some bacterioferrins that are composed of heteropolymers, in which one subunit confers haem-binding ability, while the other confers the ferroxidase activity; an example of this type are subunits A and B from *Neisseria gonorrhoeae* bacterioferritin, a situation reminiscent of that for the H and L chains in mammalian ferritins. In these cases, the subunit with the ferroxidase activity has all the ligands for the di-iron centre conserved (Andrews, 1998). Concerning the bacterial or eukaryotic ferritins, in general the two residues that are not conserved are Glu132 and His135 (in *Dd* Bfr), which are substituted, respectively, by a glutamine (which is no longer a ligand) and a glutamate (Harrison and Arosio, 1996).

Rubrerythrin, which was also reported to have some ferroxidase activity (DeMaré *et al*., 1996; Kurtz, 1997), and a variety of di-iron proteins, which have functions as diverse as the oxygenation of methane, reduction of ribonucleotides and oxygen reduction or transport (Kurtz, 1997; Rosenzweig *et al*., 1997; Tong *et al*., 1998; Frazão *et al*., 2000; Gomes *et al*., 2001), have di-iron sites with a similar geometry to that observed in *Dd* Bfr (Figure 3). The structure of the 'as isolated' *Dd* Bfr has, however, additional features at the di-iron site. Electron density bridging the two metal sites was clearly observed on the opposite side of the histidyl ligands (Macedo *et al*., 2003).

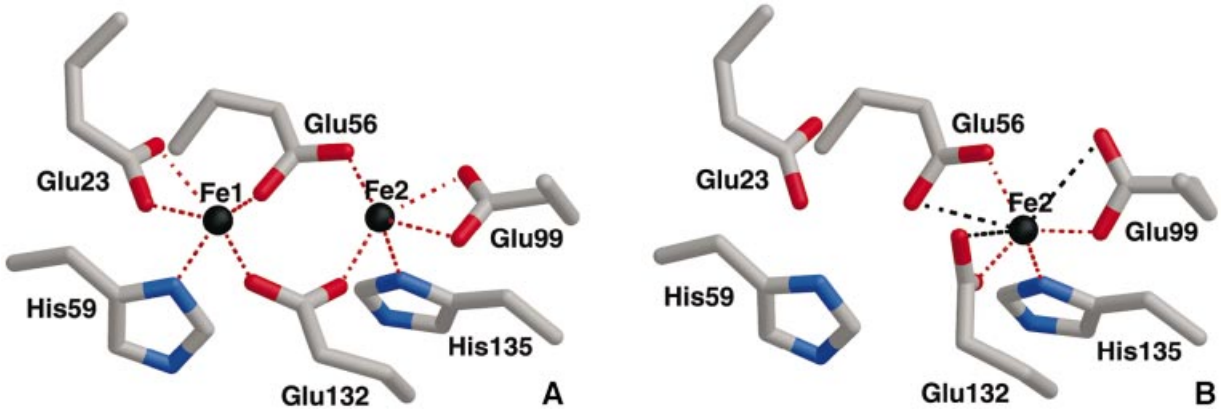

Fig. 3. The di-iron centre in *Dd* Bfr, showing the residues coordinating as terminal or bridging ligands. Red dashed lines indicate bonds, while black dashed lines indicate distances >2.60 Å. The distance between the iron atoms in the as 'isolated' structure is 3.71 Å (PDB 1nfv), while in the reduced structure it is 3.99 Å (PDB 1nf4). (**A**) View of the centre in the 'as isolated' structure with the unequivocally identified ligands. (**B**) View of the site in the 'cycled' oxidized structure (PDB 1nf6). Fe1 is strongly depleted in this structure with an occupancy between 0 and 30% in the various crystallographic independent subunits.

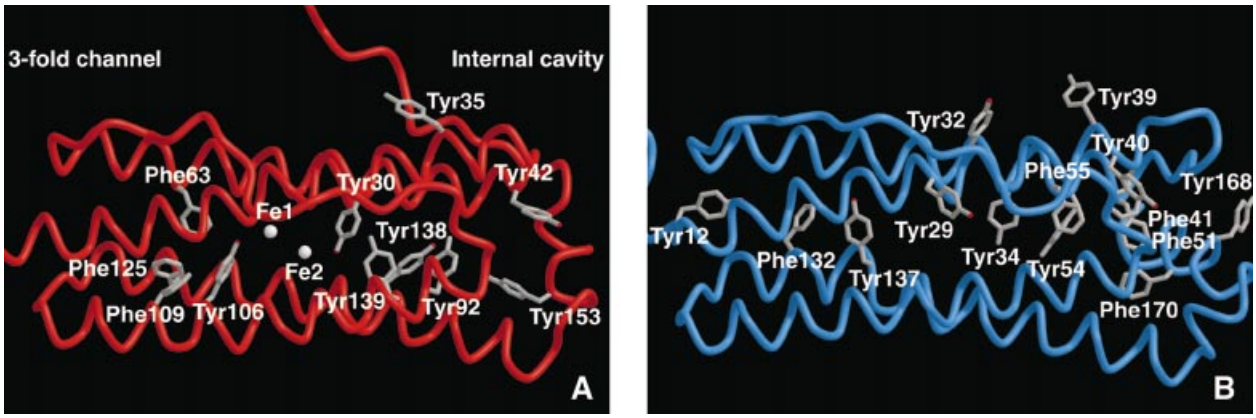

Fig. 4. Diagrams of *Dd* Bfr (**A**; PDB 1nfv) and human H chain ferritin subunits (**B**; PDB code 1fha) showing all the tyrosine and phenylalanine residues that form a possible electron transfer path from the 3-fold channel to the internal cavity of the molecule through the di-iron site.

Due to lack of resolution and probably because this sample was not in a single oxidation and/or catalytic state, this electron density could not be unequivocally assigned. However, water molecules, a peroxo intermediate and/or oxo or hydroxo bridge could be readily fitted into the density with acceptable geometries. Average iron to iron distances in *Dd* Bfr were found to be 3.71 Å in the 'as isolated' and 3.99 Å in the reduced structure (Macedo *et al*., 2003). In the case of *Ec* ferritin, the equivalent iron to iron distance is 3.24 Å (Stillman *et al*., 2001), while in *Ec* Bfr the manganese to manganese distance is 3.9 Å (Frolow and Kalb, 2001). These distances are within the range of those observed in proteins with di-iron centres (Kurtz, 1997; Frazão *et al*., 2000).

A mechanism was proposed for the oxidation of iron in *Ec* Bfr (Yang *et al*., 2000; Bou-Abdallah *et al*., 2002) and in mammalian ferritin H chain (Yang *et al*., 1998) based on the observation that oxygen peroxide is an intermediate product resulting from the reduction of molecular oxygen at the ferroxidase centre. On the other hand, spectroscopic studies in ferritins have clearly indicated that dioxygen binds to the Fe(II) pair to form diferric-peroxo intermediates (Treffry *et al*., 1995; Zhao *et al*., 1997; Moenne-Loccoz *et al*., 1999; Hwang *et al*., 2000). A recent X-ray study allowed the identification of a double oxo/hydroxo/water bridge between the iron ions in *Ec* ferritin (Stillman *et al*., 2001). Thus, it is reasonable to suggest that the structure captured in the 'as isolated' *Dd* Bfr crystal is a combination of intermediates at various stages of the ferroxidase reaction with different possible bridging ligands.

Another feature of the study of *Dd* Bfr (Macedo *et al*., 2003) was revealed by the structure of the oxidized 'cycled' sample. When the protein sample was fully reduced and subsequently allowed to oxidize in the presence of atmospheric oxygen, the ferroxidase centre appeared with Fe1 almost depleted. No sign of any bridging/terminal oxygen ligand remained in the electron density maps (in this as well as in the reduced structure), nor could a peak be assigned to an ordered iron ion elsewhere in the structure. Glu56, formerly bound to Fe1, approaches Fe2, while the carboxylate group of Glu132

undergoes a rearrangement, rotating by nearly 90° about the Cγ–Cδ bond (see Figure 3B).

The tyrosine chain

Spectroscopic experiments have implicated tyrosyl residues in iron oxidation (Waldo and Theil, 1993; Pereira *et al*., 1997; Ha *et al*., 1999), either by an Fe(III)–tyrosinate complex or tyrosine radical formation as intermediate species. In human H ferritin, a transient blue species was associated with Tyr34, a conserved residue in both mammalian ferritin subunit types and bacterioferritins. In bullfrog H ferritin, on the other hand, a purple Fe(III)–tyrosinate complex was identified by resonance Raman spectroscopy in the early stages of the biomineralization process (Waldo and Theil, 1993). It appears to be the first of a series of Fe–protein complexes as iron passes from the solution outside ferritin, through the protein coat, to the solid iron core inside the cavity. Tyr34 has been proposed as the tyrosinate Fe(III) ligand (Bauminger *et al*., 1993), but its presence in L chain subunits, combined with the fact that this Fe(III)-tyrosinate species is not detected in this type of subunit, led Waldo *et al*. (1993) to propose Tyr29 as an alternative residue on the outer surface of the molecule.

Diagrams of *Dd* Bfr (A) and human H ferritin (B) are shown in Figure 4. In *Dd* Bfr, a sequence of tyrosine and phenylalanine residues is positioned forming what appears to be an electron transfer path along the internal side of the four-helix bundle. The Phe residues are located between the 3-fold channel and the di-iron site, while most of the Tyr residues lead from the di-iron centre to the internal cavity of the molecule. Tyr30 (Tyr34 in human H ferritin) and Tyr106 (Tyr137 in human H ferritin) are located at each side of the ferroxidase centre, inside the four-helix bundle, and are accessible only through the di-iron centre and the opening into the ferritin cavity. Human H ferritin has a slightly different distribution, but the sequence of Tyr and Phe crossing the subunit is also present.

The biological relevance of this 'tyrosine chain' crossing the (bacterio)ferritin subunit with radical/intermediate tyrosine–protein complex formation and the possibility that it may constitute a route for electron transfer path during iron uptake and release remains to be determined.

The pore—a specific iron entry pathway?

Figure 5 represents views of the molecular surface of *Dd* Bfr as seen from inside the molecule, showing the presence of a pore that leads directly to the ferroxidase di-iron site. The iron atoms are located ~6 Å below the pore entrance, which is approximately circular in shape with a radius of ~1.4 Å. This pore is wider in the base, with an approximately elliptical shape, the major axis (5.3 Å) being the Fe1–Fe2 direction. The entrance and dimensions of the pore are such that species such as Fe ions or water molecules may enter and leave the pore. This pore is, in the structure of *Dd* Bfr (Macedo *et al*., 2003), formed mainly by hydrophilic residues. Such an observation prompts the hypothesis that the entry of iron can occur through this pore, to form the di-iron site. Upon reaction with oxygen, the iron atoms are oxidized and the Fe1 position is observed to be significantly depleted. Under the conditions in which this reaction was carried out, it is likely that this Fe atom may have left the di-iron site to the solvent through the pore. However, under physiological conditions, it is also possible that this Fe atom may be translocated into the inner core via a concerted movement of two residues that lie below the iron position, His59 and Glu131. In this way a continuous channel to the sphere core is opened, as shown in Figure 5D. Local pH or other factors may induce a different conformation of these residues, which can occur without any obvious stereochemical clash or interference with neighbouring residues.

Similar pores can also be found in the structures of *Ec* Bfr (Frolow *et al*., 1994), *Rc* Bfr (Cobessi *et al*., 2002) and *Ec* ferritin (Stillman *et al*., 2001). In this last case, the pore is hydrophobic, and it has been assumed to provide access for molecular oxygen and perhaps for metal atoms shielded by water. The high-resolution structure of this ferritin was described in parallel with that of its Fe(III) derivative. The three iron ions observed in the structure were inserted in the molecule by aerobic soaking of the crystals of the apo-protein in a ferrous salt solution. Two of these atoms (A and B) formed the di-iron site. Iron B has a lower occupancy (70%) than that of the other two iron positions. This has been interpreted by the authors (Stillman *et al*., 2001) as a loss of this oxidized site, induced by the eventual movement of the iron ion from this position into the inner protein cavity. The third ion (C) penetrated as far as the inner surface of the protein shell, where it coordinates four glutamate carboxylates and two water molecules (Stillman *et al*., 2001). Coordination of iron in this position appears to have been accomplished, by comparison with the structure of the apo-protein, with the help of a large movement undergone by His46. This residue is close to the di-iron site and a small adjustment in the orientation of Glu49, a residue close to His46 and at the inner surface of the protein core, is also required. Mutations of the iron C glutamate ligands to alanines resulted in loss of iron in this nucleation site, but promoted core formation rather than diminishing it (Stillman *et al*., 2001). The much less bulkier alanine ligands in the mutants may have allowed an easier access to the inner cavity, where the iron ions are possibly distributed between multiple sites. Thus, it is reasonable to speculate that the iron ions entered through the pore on the external surface, formed the di-iron site and from there eventually moved into the inner protein core.

The observations mentioned in the structures of the apo and iron-loaded *Ec* ferritin support the hypothesis formulated above for the putative channel through the protein shell in *Dd* Bfr. It is interesting to note that the His46 in *Ec* ferritin is conserved in the known prokaryote non-haem ferritins, while His59 in *Dd* Bfr is also a conserved residue among most bacterioferritins. These two histidines are in both cases close to the di-iron site, but they are not in corresponding positions in the respective structures. Thus, in addition to being involved with metal binding to the di-iron site, they may have a gating role for the passage of iron into or out of this site.

Together, the structural results obtained with the *Ec* ferritin and the three catalytic states of the *Dd* Bfr structures indicate a possible alternative route for iron uptake through the protein shell, as opposed to access through the 3- or 4-fold axis channels. Such a mechanism,

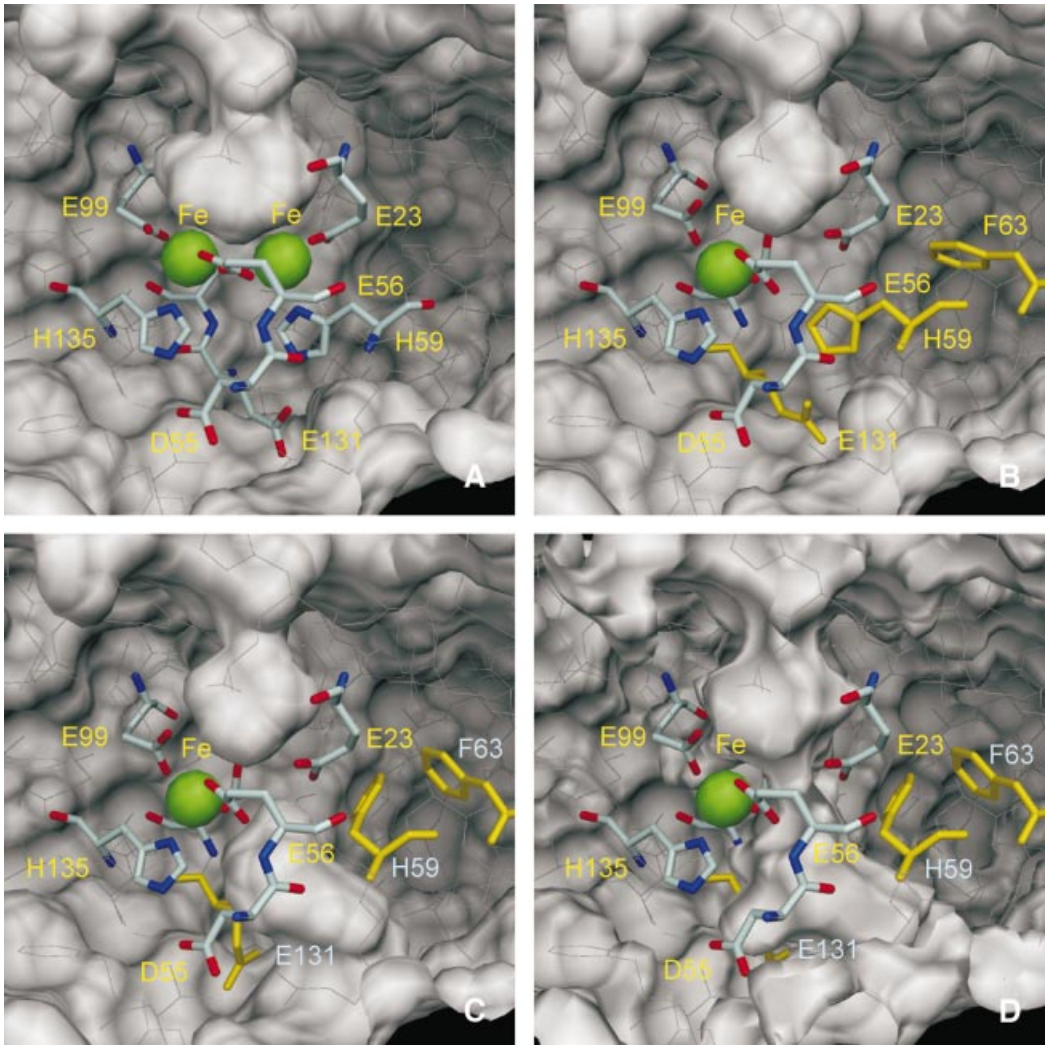

Fig. 5. The molecular surface of the *Dd* Bfr homodimer (PDB 1nfv), viewed from inside the molecule, near the di-iron centre. The iron atoms are represented as green spheres with 1.30 Å radius, and the residues that coordinate the iron atoms are drawn as sticks. Asp55 and Glu131, which form hydrogen bonds with iron-coordinating residues His135 and His59, respectively, are also drawn as sticks. Glu132, which bridges the di-iron centre, is partly hidden and is not labelled for clarity. The remaining residues in the Bfr homodimer are drawn as thin white lines. The outside surface of the homodimer is near the top of the figures, while the interior surface is near the bottom. A pocket in the external surface is clearly visible in all views. This pocket is larger in the 'native' (not shown) and reduced Bfr (**A**; PDB 1nf4) than in the oxidized 'cycled' structure (**B**; PDB 1nf6). (**C**) The hypothetical side-chain motions of His59, Phe63 and Glu131 (drawn in yellow) in the oxidized Bfr structure, which form a channel that allows access from the depleted iron site to the inside of the Bfr 24mer. A small pocket in the internal surface can be seen in (A) and (B) just below His59, which may be the precursor of this hypothetical access channel. In (A–C), the molecular surfaces were calculated with a 1.35 Å probe radius. In (**D**), the molecular surface was calculated with a 0.8 Å probe radius, and a channel that may allow a Fe^{2+} ion (radius 0.76 Å) to cross the protein shell is visible. The molecular surfaces were calculated with program MSMS (Sanner *et al*., 1996) and the figures were prepared with DINO (Philippsen, 2002).

involving the participation and restoration of the native di-iron centre, is clearly specific for iron, in accordance with what is known in terms of iron uptake by (bacterio)ferritins, and has the advantage of coupling uptake with the ferroxidase activity.

Electrostatic calculations: the 3- and 4-fold axis channels

Entry and exit paths for iron atoms have been mainly postulated through the 3- and 4-fold axis protein channels (Theil *et al*., 2000; Theil, 2001). Several types of ions have been identified at these sites from crystal soaking experiments in (bacterio)ferritins (Frolow *et al*., 1994; Harrison *et al*., 1998; Cobessi *et al*., 2002).

The 3-fold axis channels are normally of hydrophilic character, a property conserved in mammalian ferritins. The 4-fold axis interface is highly hydrophobic in mammalian L ferritins, while H ferritins have some histidine and methionine residues pointing towards either side of the protein coat (Crichton, 2001). In invertebrates, plants and bacteria, however, some variation is observed (Banyard *et al*., 1978); for example, *Ec* Bfr exhibits hydrophilic 4-fold axis channels (Frolow *et al*., 1993).

Support for the 3-fold axis entry route for positive ions has come from calculations of electrostatic potentials in human H ferritin (Douglas and Ripoll, 1998), which show

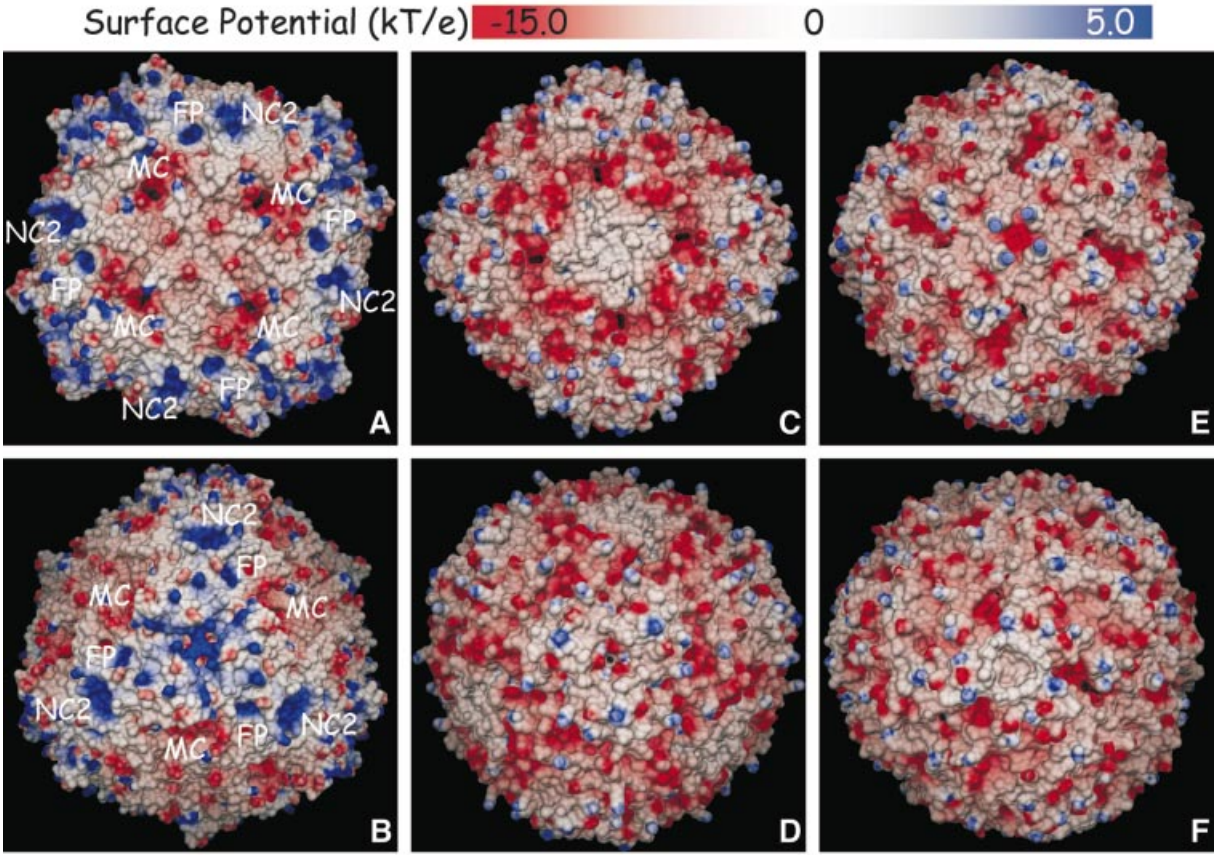

Fig. 6. Electrostatic potential surfaces of *Dd* Bfr (**A** and **B**; PDB 1nfv), *Ec* Bfr (**C** and **D**; PDB 1bcf) and *Ec* ferritin (**E** and **F**; PDB 1eum). (A, C and E) Views down a 4-fold axis (non-crystallographic). (B, D and F) Views down a 3-fold axis (crystallographic for *Dd* Bfr, non-crystallographic for *Ec* Bfr and *Ec* ferritin). The molecular surfaces were calculated with MSMS (Sanner *et al*., 1996) using a probe radius of 1.4 Å (1.2 Å for *Ec* Bfr). The electrostatic potentials were calculated with MEAD (Bashford, 1997) using protein and external dielectric constants of 4 and 80, respectively, a temperature of 300 K and an ionic strength of 0.1 M; for *Dd* Bfr, +3 charges were assumed for all the iron atoms; for *Ec* Bfr, +2 charges were assumed for the manganese atoms and +3 for the haem iron atoms; for *Ec* ferritin, no metal ions were included in the calculations as none is present in the deposited coordinates. FP, ferroxidase pore; MC, major channel; NC2, 2-fold non-crystallographic axis.

that the negative outer entrance is surrounded by patches of positive potential and this arrangement leads to electrostatic fields directing cations towards the channel entrance (Chasteen and Harrison, 1999).

A comparison of the external molecular surfaces and electrostatic potentials calculated for five proteins using the same methodology, three from bacteria (*Dd* Bfr, *Ec* Bfr and *Ec* ferritin) and two mammalian proteins (horse spleen ferritin and human H-chain ferritin), is represented in Figures 6 and 7, respectively. Overall, *Dd* Bfr shows many more positive surface regions than the other two bacterial proteins. In addition, it is the only molecule for which the fully occupied ferroxidase centre was considered in the calculations. Indeed, the electrostatic potential surface near the ferroxidase pocket (site FP in Figure 6) is strongly positive. When similar calculations are carried out for the reduced and the 'cycled' Bfr structures (not shown), a gradual shift of this electrostatic potential surface towards negative values is observed, since the negative charges of the surrounding glutamic acid residues gradually override the positive charges of the two Fe(II) atoms in the reduced structure, and of the single Fe(III) atom in the 'cycled' structure. Site NC2 is another region of positive charges on the surface of *Dd* Bfr, which are due to the presence of four surface lysine residues, a situation only observed for *Dd* Bfr.

However, it is clear from Figure 6 that clusters of negative charges appear in the bacterial proteins around MC channels, which are different from those at the 3- or 4-fold axis channels, and extend to the interior of the protein shells. These channels are sufficiently large to admit the entry of iron ions into the inner core of the proteins. In contrast, their appearance in mammalian ferritins can only be postulated through conformational modifications on the corresponding surface residues.

Our calculations performed on the mammalian ferritins (Figure 7) are in accordance with those reported previously by Douglas and Ripoll (1998), indicating that the outer regions with negative potentials are localized around the 3-fold channels, which also cross the protein shell up to the inner core. These 3-fold channel entrances are surrounded by regions of positive surface electrostatic potential, a situation also observed in the horse spleen ferritin structure.

In addition to an iron entry path in mammalian ferritins, the 3-fold channel appears to be a dynamic aperture with a 'shutter' that cytoplasmic factors might open or close to regulate iron uptake *in vivo* (Takagi *et al*., 1998).

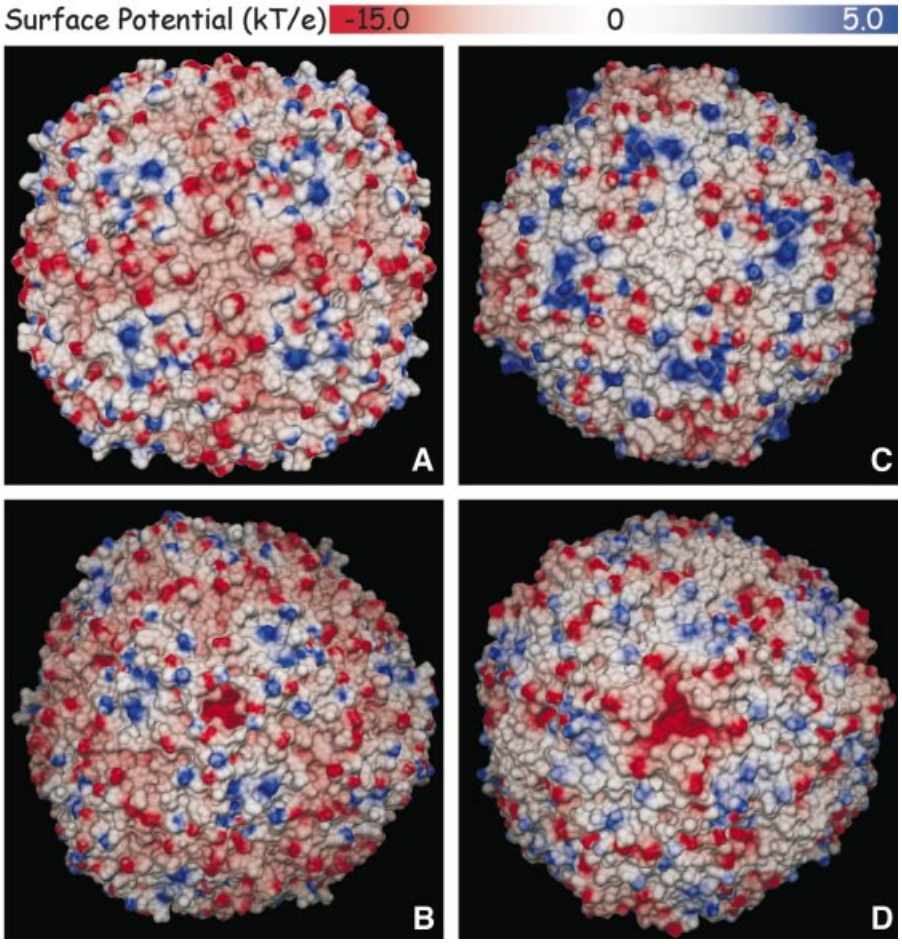

Fig. 7. Electrostatic potential surfaces of human H chain ferritin (**A** and **B**; PDB 2fha) and native horse spleen ferritin (**C** and **D**; PDB 1ier). (A and C) Views down a crystallographic 4-fold axis. (B and D) Views down a 3-fold crystallographic axis. The molecular surfaces were calculated with MSMS (Sanner *et al*., 1996) using a probe radius of 1.4 Å. The electrostatic potentials were calculated with MEAD (Bashford, 1997) using protein and external dielectric constants of 4 and 80, respectively, a temperature of 300 K and an ionic strength of 0.1 M; none of the metal ions present in the deposited coordinates (Ca^{2+} for 2fha, Cd^{2+} for 1ier) was included in the calculations.

Mutations around the 3-fold pore have been shown to have a dramatic effect in the rate of iron release. This suggests that there might be biological ferritin 'unfolders' which regulate iron release from ferritin (Theil *et al*., 2000).

This situation contrasts to what is observed in the bacterial ferritins, where no negatively charged 3-fold channel is observed. Indeed, in *Dd* Bfr the entrance to the 3-fold channel is mostly positively charged on either side of the protein coat. In the case of the bacterial ferritins, the MC channels now described may take the role of the 3-fold channel for iron uptake, as proposed for mammalian ferritins.

Conclusions

The evidence to date for bacterioferritins has indicated that at least in one case, that of *Dd* Bfr, the protein has a di-iron centre *in vivo*. Furthermore, this centre seems to be involved in the ferroxidase reaction in all ferritins, a fact that has already been postulated by the observation of peroxo-differic intermediates. Structural evidence of these intermediates was provided by biochemical and spectroscopic studies on several proteins and EXAFS studies on recombinant frog M ferritin. X-ray diffraction studies indicated the possibility of the existence of oxo/peroxo intermediates in the cases of *Ec* ferritin and *Dd* Bfr. Specific entries for iron, consistent with the ferroxidase reaction, were considered through pores above the di-iron sites in *Dd* Bfr and in the loaded form of *Ec* ferritin. Additional channels in bacterioferritins and the 3-fold channels in ferritins may provide direct routes for iron by the mineralization reaction, once the initial nucleation sites are established inside the protein core.

Acknowledgements

The author thanks Sofia Macedo and Pedro Matias for the prepartion of the drawings presented in this review. António Xavier is thanked for helpful discussions, and Peter Lindley, Célia Romão and Miguel Teixeira for discussion and a critical reading of the manuscript. Thanks are due to the ESRF, Grenoble (France), for the provision of synchrotron radiation.

References

Andrews,S.C. (1998) Iron storage in bacteria. *Adv. Microb. Physiol.*, **40**, 281–351.

Arosio,P. and Levi,S. (2002) Ferritin, iron homeostasis, and oxidative damage. *Free Rad. Biol. Med.*, **33**, 457–463.

Banyard,S.H., Stammers,D.K. and Harrison,P.M. (1978) Electron density map of apoferritin at 2.8 Å resolution. *Nature*, **271**, 282–284.

Bashford,D. (1997) An object-oriented programming suite for electrostatic effects in biological molecules. In *Scientific Computing in Object-Oriented Parallel Environments.* Vol. 1343. Springer, Berlin, Germany, pp. 233–240.

Bauminger,E.R., Harrison,P.M., Hechel,D., Hodson,N.W., Nowik,I., Treffry,A. and Yewdall,S.J. (1993) Iron (II) oxidation and early intermediates of iron-core formation in recombinant human H-chain ferritin. *Biochem. J.*, **296**, 709–719.

Bou-Abdallah,F., Lewin,A.C., Le Brun,N.E., Moore,G.R. and Chasteen,N.D. (2002) Iron detoxification properties of *Escherichia coli* bacterioferritin. Attenuation of oxyradical chemistry. *J. Biol. Chem.*, **277**, 37064–37069.

Chasteen,N.D. and Harrison,P.M. (1999) Mineralization in ferritin: an efficient means of iron storage. *J. Struct. Biol.*, **126**, 182–194.

Cobessi,D., Huang,L.S., Ban,M., Pon,N.G., Daldal,F. and Berry,E.A. (2002) The 2.6 Å resolution structure of *Rhodobacter capsulatus* bacterioferritin with metal-free dinuclear site and heme iron in a crystallographic 'special position'. *Acta Crystallogr. D*, **58**, 29–38.

Crichton,R. (2001) Intracellular iron storage and biomineralization. In *Inorganic Biochemistry of Iron Metabolism: From Molecular Mechanisms to Clinical Consequences*, 2nd edn. John Wiley, Chichester, UK, pp. 133–165.

Crichton,R.R. and Roman,F. (1978) Novel mechanism for ferritin iron oxidation and deposition. *J. Mol. Catal.*, **4**, 75–82.

Dautant,A., Meyer,J.B., Yariv,J., Precigoux,G., Sweet,R.M., Kalb,A.J. and Frolow,F. (1998) Structure of a monoclinic crystal from of cyctochrome b_1 (bacterioferritin) from *E.coli*. *Acta Crystallogr. D*, **54**, 16–24.

DeMaré,F., Kurtz,D.M. and Nordlund,P. (1996) The structure of *Desulfovibrio vulgaris* rubrerythrin reveals a unique combination of rubredoxin-like FeS4 and ferritin-like diiron domains. *Nat. Struct. Biol.*, **3**, 539–546.

Douglas,T. and Ripoll,D.R. (1998) Calculated electrostatic gradients in recombinant human H-chain ferritin. *Protein Sci.*, **7**, 1083–1091.

Frazão,C. *et al.* (2000) Structure of a dioxygen reduction enzyme from *Desulfovibrio gigas*. *Nat. Struct. Biol.*, **7**, 1041–1045.

Frolow,F. and Kalb,A.J. (2001) Cytochrome b_1—bacterioferritin. In Messerschmidt,A.H.R., Poulos,K. and Weighardt,K. (eds), *Handbook of Metalloproteins*. Vol. 2. Wiley, Chichester, UK, pp. 782–790.

Frolow,F., Kalb,A.J. and Yariv,J. (1993) Location of haem in bacterioferritin of *E.coli*. *Acta Crystallogr. D*, **49**, 597–600.

Frolow,F., Kalb,A.J. and Yariv,J. (1994) Structure of a unique twofold symmetric haem-binding site. *Nat. Struct. Biol.*, **1**, 453–460.

Gallois,B. *et al.* (1997) X-ray structure of recombinant horse L chain apoferritin at 2.0 Å resolution: implications for stability and function. *J. Biol. Inorg. Chem.*, **2**, 360–367.

Gomes,C.M., Le Gall,J., Xavier,A.V. and Teixeira,M. (2001) Could a diiron-containing four-helix-bundle protein have been a primitive oxygen reductase? *Chembiochem*, **2**, 583–587.

Granier,T., Gallois,B., Langlois d'Estaintot,B., Dautant,A., Chevalier,J.M., Mellado,J.M., Beaumont,C., Santambrogio,P., Arosio,P. and Precigoux,G. (2001) Structure of mouse L-chain ferritin at 1.6 Å resolution. *Acta Crystallogr. D*, **57**, 1491–1497.

Granier,T., Langlois D'Estaintot,B., Gallois,B., Chevalier,J.M., Precigoux,G., Santambrogio,P. and Arosio,P. (2003) Structural description of the active sites of mouse L-chain ferritin at 1.2 Å resolution. *J. Biol. Inorg. Chem.*, **8**, 105–111.

Grant,R.A., Filman,D.J., Finkel,S.E., Kolter,R. and Hogle,J.M. (1998) The crystal structure of Dps, a ferritin homolog that binds and protects DNA. *Nat. Struct. Biol.*, **5**, 294–303.

Ha,Y., Shi,D., Small,G.W., Theil,E.C. and Allewell,N.M. (1999) Crystal structure of bullfrog M ferritin at 2.8 Å resolution: analysis of subunit interactions and the binuclear metal center. *J. Biol. Inorg. Chem.*, **4**, 243–256.

Harrison,P.M. and Arosio,P. (1996) The ferritins: molecular properties, iron storage function and cellular regulation. *Biochim. Biophys. Acta*, **1275**, 161–203.

Harrison,P.M., Ford,G.C., Rice,D.W., Smith,J.M., Treffry,A. and White,J.L. (1987) Structural and functional studies on ferritins. *Biochem. Soc. Trans*, **15**, 744–748.

Harrison,P.M., Hempstead,P.D., Artymiuk,P.J. and Andrews,S.C. (1998) Structure–function relationships in the ferritins. *Met. Ions Biol. Syst.*, **35**, 435–477.

Hempstead,P.D., Hudson,A.J., Artymiuk,P.J., Andrews,S.C., Banfield,M.J., Guest,J.R. and Harrison,P.M. (1994) Direct observation of the iron binding sites in a ferritin. *FEBS Lett.*, **350**, 258–262.

Hempstead,P.D., Yewdall,S.J., Fernie,A.R., Lawson,D.M., Artymiuk,P.J., Rice,D.W., Ford,G.C. and Harrison,P.M. (1997) Comparison of the three-dimensional structures of recombinant human H and horse L ferritins at high resolution. *J. Mol. Biol.*, **268**, 424–448.

Hwang,J., Krebs,C., Huynh,B.H., Edmondson,D.E., Theil,E.C. and Penner-Hahn,J.E. (2000) A short Fe–Fe distance in peroxodiferric ferritin: control of Fe substrate versus cofactor decay? *Science*, **287**, 122–125.

Ilari,A., Stefanini,S., Chiancone,E. and Tsernoglou,D. (2000) The dodecameric ferritin from *Listeria* innocua contains a novel intersubunit iron-binding site. *Nat. Struct. Biol.*, **7**, 38–43.

Kleywegt,G.J. and Jones,T.A. (1999) Software for handling macromolecular envelopes. *Acta Crystallogr. D*, **55**, 941–944.

Kurtz,J.D.M. (1997) Structural similarity and functional diversity in diiron-oxo proteins. *J. Biol. Inorg. Chem.*, **2**, 159–167.

Lawson,D.M. (1990) X-ray structure determination of recombinant ferritins. PhD thesis, University of Sheffield, Sheffield, UK.

Lawson,D.M. *et al.* (1991) Solving the structure of human H ferritin by genetically engineering intermolecular crystal contacts. *Nature*, **349**, 541–544.

Le Brun,N.E., Wilson,M.T., Andrews,S.C., Guest,J.R., Harrison,P.M., Thomson,A.J. and Moore,G.R. (1993) Kinetic and structural characterization of an intermediate in the biomineralization of bacterioferritin. *FEBS Lett.*, **333**, 197–202.

Le Brun,N.E., Andrews,S.C., Guest,J.R., Harrison,P.M., Moore,G.R. and Thomson,A.J. (1995) Identification of the ferroxidase centre of *Escherichia coli* bacterioferritin. *Biochem. J.*, **312**, 385–392.

Levi,S., Corsi,B., Bosisio,M., Invernizzi,R., Volz,A., Sanford,D., Arosio,P. and Drysdale,J. (2001) A human mitochondrial ferritin encoded by an intronless gene. *J. Biol. Chem.*, **270**, 24437–24440.

Macedo,S. *et al.* (2003) The nature of the di-iron site in the bacterioferritin from *Desulfovibrio desulfuricans*. *Nat. Struct. Biol.*, **10**, 285–290.

Moenne-Loccoz,P., Krebs,C., Herlihy,K., Edmondson,D.E., Theil,E.C., Huynh,B.H. and Loehr,T.M. (1999) The ferroxidase reaction of ferritin reveals a diferric μ-1,2 bridging peroxide intermediate in common with other O_2-activating non-heme diiron proteins. *Biochemistry*, **38**, 5290–5295.

Papinutto,E., Dundon,W.G., Pitulis,N., Battistutta,R., Montecucco,C. and Zanotti,G. (2002) Structure of two iron-binding proteins from *Bacillus anthracis*. *J. Biol. Chem.*, **277**, 15093–15098.

Pereira,A.S., Tavares,P., Lloyd,S.G., Danger,D., Edmondson,D.E., Theil,E.C. and Huynh,B.H. (1997) Rapid and parallel formation of Fe^{3+} multimers, including a trimer, during H-type subunit ferritin mineralization. *Biochemistry*, **36**, 7917–7927.

Pereira,A.S., Small,W., Krebs,C., Tavares,P., Edmondson,D.E., Theil,E.C. and Huynh,B.H. (1998) Direct spectroscopic and kinetic evidence for the involvement of a peroxodiferric intermediate during the ferroxidase reaction in fast ferritin mineralization. *Biochemistry*, **37**, 9871–9876.

Philippsen,A. (2002) DINO: visualizing structural biology. http://www.dino3d.org.

Rice,D.W., Ford,G.C., White,J.L., Smith,J.M.A. and Harrison,P.M. (1983) The spatial structure of horse spleen apoferritin. *Adv. Inorg. Biochem.*, **5**, 39–50.

Romão,C.V., Louro,R., Timkovich,R., Lubben,M., Liu,M.Y., LeGall,J., Xavier,A.V. and Teixeira,M. (2000a) Iron-coproporphyrin III is a natural cofactor in bacterioferritin from the anaerobic bacterium *Desulfovibrio desulfuricans*. *FEBS Lett.*, **480**, 213–216.

Romão,C.V., Regalla,M., Xavier,A.V., Teixeira,M., Liu,M.Y. and Le Gall,J. (2000b) A bacterioferritin from the strict anaerobe *Desulfovibrio desulfuricans* ATCC 27774. *Biochemistry*, **39**, 6841–6849.

Rosenzweig,A.C., Brandstetter,H., Whittington,D.A., Nordlund,P., Lippard,S.J. and Frederick,C.A. (1997) Crystal structures of the methane monooxygenase hydroxylase from *Methylococcus capsulatus* (Bath): implications for substrate gating and component interactions. *Proteins*, **29**, 141–152.

Sanner,M.F., Spehner,J.C. and Olson,A.J. (1996) Reduced surface: an efficient way to compute molecular surfaces. *Biopolymers*, **38**, 305–320.

Stillman,T.J., Hempstead,P.D., Artymiuk,P.J., Andrews,S.C., Hudson,A.J., Treffry,A., Guest,J.R. and Harrison,P.M. (2001) The high-resolution X-ray crystallographic structure of the ferritin

(EcFtnA) of *Escherichia coli*; comparison with human H ferritin (HuHF) and the structures of the Fe^{3+} and Zn^{2+} derivatives. *J. Mol. Biol.*, **307**, 587–603.

Takagi,H., Shi,D., Ha,Y., Allewell,N.M. and Theil,E.C. (1998) Localized unfolding at the junction of three ferritin subunits. A mechanism for iron release? *J. Biol. Chem.*, **273**, 18685–18688.

Theil,E.C. (2001) Ferritin. In Messerschmidt,A., Poulos,H.R. and Weighardt,K. (eds), *Handbook of Metalloproteins*. Vol. 2. Wiley, Chichester, UK, pp. 771–781.

Theil,E.C., Takagi,H., Small,G.W., He,L., Tipton,A.R. and Danger,D. (2000) The ferritin iron entry and exit problem. *Inorg. Chim. Acta*, **297**, 242–251.

Tong,W. *et al*. (1998) Characterization of Y122F R2 of *Escherichia coli* ribonucleotide reductase by time-resolved physical biochemical methods and X-ray crystallography. *Biochemistry*, **37**, 5840–5848.

Treffry,A., Zhao,Z., Quail,M.A., Guest,J.R. and Harrison,P.M. (1995) Iron(II) oxidation by H chain ferritin: evidence from site-directed mutagenesis that a transient blue species is formed at the dinuclear iron center. *Biochemistry*, **34**, 15204–15213.

Trikha,J., Waldo,G.S., Lewandowski,F.A., Ha,Y., Theil,E.C., Weber,P.C. and Allewell,N.M. (1994) Crystallization and structural analysis of bullfrog red cell L-subunit ferritins. *Proteins*, **18**, 107–118.

Waldo,G.S. and Theil,E.C. (1993) Formation of iron(III)–tyrosinate is the fastest reaction observed in ferritin. *Biochemistry*, **32**, 13262–13269.

Waldo,G.S., Ling,J., Sanders-Loehr,J. and Theil,E.C. (1993) Formation of an Fe(III)–tyrosinate complex during biomineralization of H-subunit ferritin. *Science*, **259**, 796–798.

Yang,X., Chen-Barrett,Y., Arosio,P. and Chasteen,N.D. (1998) Reaction paths of iron oxidation and hydrolysis in horse spleen and recombinant human ferritins. *Biochemistry*, **37**, 9743–9750.

Yang,X., Le Brun,N.E., Thomson,A.J., Moore,G.R. and Chasteen,N.D. (2000) The iron oxidation and hydrolysis chemistry of *Escherichia coli* bacterioferritin. *Biochemistry*, **39**, 4915–4923.

Zhao,Z., Treffry,A., Quail,M.A., Guest,J.R. and Harrison,P.M. (1997) Catalytic iron (II) oxidation in the non-haem ferritin of *Escherichia coli*: the early intermediate is not an iron tyrosinate. *J. Chem. Soc. Dalton Trans.*, **21**, 3977–3978.

Received December 4, 2002; revised March 7, 2003;
accepted March 12, 2003